Available online at www.sciencedirect.com

Journal of Applied Research and Technology

Journal of Applied Research and Technology 15 (2017) 454–463

www.jart.ccadet.unam.mx

Original

Fixed bed adsorption of tetracycline on a mesoporous activated carbon: Experimental study and neuro-fuzzy modeling

Mojtaba Hedayati Marzbali, Mohamad Esmaieli *

Center for Separation Process Modeling and Nano-Computations, School of Chemical Engineering, College of Engineering, University of Tehran, P.O. Box 11365-4563, Iran

Received 10 January 2017; accepted 9 May 2017
Available online 7 October 2017

Abstract

This study investigates the use of synthesized mesoporous carbon in the fixed bed adsorption, as a promising process, to eliminate tetracycline from wastewater. In order to study the adsorptive capability of adsorbent, particles were embedded in a laboratory-scale Pyrex glass tube. An increase in initial concentration and decrease in bed height and flow rate led to the higher adsorption capacity. The highest bed capacity of 76.97 mg g^{-1} was obtained using 4 cm bed depth, 4 mL min^{-1} and 50 mg L^{-1} influent concentration. The initial part of breakthrough curve perfectly matched the Adams–Bohart model at all experimental conditions. However, it was anticipated that Yoon–Nelson model could predict the whole curve acceptably, the results showed an inaccurate fitting. Therefore, the adaptive neuro-fuzzy inference system (ANFIS) was used to predict the breakthrough curve using data series of adsorption experiments. This model indicated a good statistical prediction in terms of relative errors.

Keywords: Apricot shell; Tetracycline; Column adsorption; Machine learning; Neuro-fuzzy

1. Introduction

Only three percent of the water found on the earth's surface is freshwater and a large amount of that is locked up in glaciers, ice caps and permanent snow. The remaining freshwater is in groundwater, lakes and rivers which is used for agriculture, industry and so on. But regrettably, such activities can contaminate freshwater by a large variety of potentially perilous substances. The most important risk from the presence of these pollutants in surface water is the long-term harmful consequences on various ecosystems, including acute and chronic toxicity (González-Pleiter et al., 2013). In spite of successful effect of antibiotics in veterinary and human medicine treating bacterial and protozoan infections and as additives in animal foodstuffs, their residues in the water can cause antimicrobial resistance genes (ARGs), even at relatively low concentrations (Xu et al., 2016). The transformation and migration of these ARGs in the ecosystem is potentially more harmful than the antibiotic residues in the environment (Chen, Zheng, Zhou, & Zhao, 2017). According to the WHO projection, they will cause dying of 10 million people annually by 2050; consequently this threatening pollutant is considered as one of the most important health concerns of the current century (He et al., 2016). The concentrations for antibiotic residue in the hospital and pharmaceutical manufacturing wastewater have been reported usually up to 100 to 500 mg L^{-1} (Larsson, de Pedro, & Paxeus, 2007).

Adsorption by porous materials has been widely considered to be the most promising and robust method in eliminating antibiotics from wastewater due to its low cost, simplicity, fastness, high efficiency as well as environmental friendliness (Marzbali, Mir, Pazoki, Pourjamshidian, & Tabeshnia, 2017). Furthermore, producing low-cost adsorbent by agricultural waste as a raw material, makes adsorption an operational process (Martins et al., 2015). The continuous fixed bed mode peruses the practical application of the adsorption process. Moreover, several advantages like simple operation, high yield and easy scale up from a laboratory-scale distinguish this process from batch mode adsorption (Oguz, 2013).

* Corresponding author.
E-mail address: esmaili@ut.ac.ir (M. Esmaieli).

Peer Review under the responsibility of Universidad Nacional Autónoma de México.

http://dx.doi.org/10.1016/j.jart.2017.05.003

Common methods in chemical processes usually have limitations of complexity and nonlinearity in their systems. Among different techniques proposed to these processes, adaptive neuro-fuzzy inference system (ANFIS) is highly recommended; this is not only because it does not need governing chemical and physical laws of processes, but also due to this fact that once it is developed and trained, ANFIS model can easily predict the output of system for further designation of chemical processes (Cole, Powell, & Edgar, 2012; Pirdashti, Curteanu, Kamangar, Hassim, & Khatami, 2013; Shacham & Brauner, 2008). The neuro-fuzzy approach has recently been developed to predict Pb(II) adsorption by ostrich bone (Amiri, Abedi-Koupai, Eslamian, Mousavi, & Hasheminejad, 2013), methane adsorption on zeolites (Rezaei, Rahmati, & Modarress, 2015) and Cu(II) removal from Leachate (Turan & Ozgonenel, 2013).

Consequently, this work aims to study tetracycline removal from aqueous solution by synthesized apricot shell-activated carbon in a continuous adsorption system. We have investigated the effects of flow rate, influent concentration and bed depth on tetracycline uptake by the produced adsorbent in a laboratory scale fixed-bed column. In addition, a model based on ANFIS system has been designed to predict tetracycline adsorption as a function of empirical parameters.

2. Experimental

2.1. Materials

Phosphoric acid with a purity of 85% was purchased from the Merck Company. The precursor, apricot nut shell from Iranian local fruit, was chosen as a raw material for production of adsorbent. Initially the shells were cleaned and washed with hot distilled water in order to remove dust-like impurities and then were dried in air oven at 80 °C for 24 h. Subsequently, the shells were ground in a mill and sieved to the desired particle size (≈ 500 μm). The sample kept in a closed bottle for further experiments. Hydrochloride salt of tetracycline (>97%) used in this study was purchased from Sinadaro Pharmaceutical Company (Tehran, Iran) and was used without further purification. The properties of tetracycline hydrochloride are listed in Table 1. All drug stock solutions were prepared by dissolving accurately weighed drug in high-purity water for needed concentrations.

2.2. Adsorbent preparation and characterization

The nanoporous activated carbon was prepared from the carbonaceous material as follows: Firstly, the raw material (5 g) was immersed into the prepared phosphoric acid at a 1:1 impregnation weight ratio under magnetic stirring for 24 h, and then the mixture was dried in oven at 100 °C for 2 h. The dried mixture was placed in an electrical furnace with a length of 25 cm and a diameter of 3 cm, which was heated at the rate of 7 °C min^{-1} until it reached 400 °C, and then maintained for 90 min under nitrogen flow of 200 mL min^{-1}. After the activation, the sample was cooled down to room temperature and was washed several times with hot distilled water until the filtrated solution reached pH 6.5. This was done to remove the remaining phosphoric acid and also other inorganic species that might be formed during the process (Martins et al., 2015). Finally, the sample was placed in an air oven (at 80 °C for 24 h) for complete drying. The comprehensive description of production stages was presented in our previous study (Marzbali, Esmaieli, Abolghasemi, & Marzbali, 2016). The activated carbon yield was calculated based on following equation:

$$yield(\%) = \frac{W_{AC}}{W_{AS}} \quad (1)$$

where W_{AC} (g) is the dry weight of final activated carbon and W_{AS} (g) is the dry weight of apricot stone.

The produced adsorbent was characterized by several analyzes. The Brunauer–Emmett–Teller (BET) method was applied to study the surface area and porosity of activated carbon. This analysis was carried out by N_2 adsorption–desorption isotherms at 77 K using Quadra Chrome adsorption instrument. The surface area was calculated by linear part of BET plot in the relative pressure ranged between 0.05 and 0.25. Moreover, the microscopic features of the raw material and derived adsorbent were studied by the Field Emission Scanning Electron Microscopy (FE-SEM).

2.3. Fixed bed column experiments

The fixed-bed mode is more similar to practical wastewater treatment and presents useful adsorption properties of a newly developed adsorbent. The fixed bed adsorption experiments were carried out in a laboratory-scale glass column with an inner diameter of 5 mm and 20 cm of length. The prepared adsorbent was packed in the column, with glass wool layer at both ends of the bed to ensure a good liquid distribution. It should be noted that tetracycline adsorption by glass wool is inconsiderable. The drug stock solution was pumped into the bed in an upward direction using a peristaltic pump (Fig. 1). The experiments were done at different bed heights (2–6 cm), influent tetracycline concentrations (20–80 mg L^{-1}) and influent flow rates (4–8 mL min^{-1}). The pH of inlet solution was set at 5, as an optimum value, which was obtained in our previous study (Marzbali et al., 2016). After beginning the process, the effluent sample was collected at regular time intervals, centrifuged at 3000 rpm for 1 h and then analyzed to obtain effluent concentration. For analysis, several specified concentrations of

Table 1
Characteristics of tetracycline.

Compound	Chemical formula	Color	Water solubility[a] (g L^{-1})		Molecular weight[a] (g mol^{-1})
TC·HCl	$C_{22}H_{24}N_2O_8$·HCl	Yellow crystalline powder	50	@ 72 °F	480.8955

[a] Data from CAMEO Chemicals (http://cameochemicals.noaa.gov/chemical/18230).

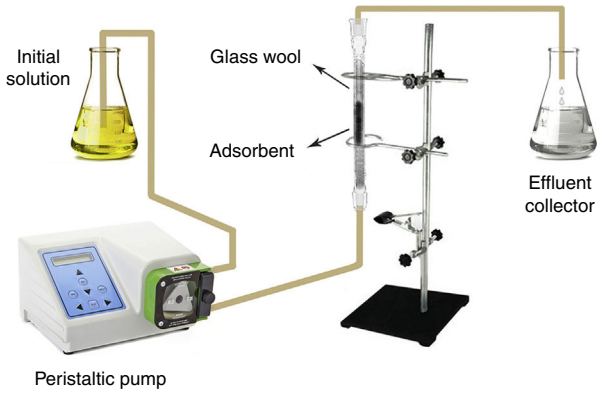

Fig. 1. A schematic of the fixed bed column.

tetracycline were placed in the UV–vis spectrophotometer and their relevant percentage of light absorbance were determined at wavelength (y_{max}) of 274 nm. Afterwards, an accurate calibration curve was obtained. The unknown tetracycline solution was placed in UV–vis spectrophotometer and its light absorbance was read. Finally, its concentration was easily calculated using calibration curve.

2.4. Column data analysis

The laboratory scale column was used to measure the parameters before applying the process to an industrial column. The experimental results were analyzed and then breakthrough curves were drawn. These curves indicate the loading behavior of tetracycline to be removed from solution in a fixed bed column (Nazari, Abolghasemi, Esmaieli, & Pouya, 2016). The area under the breakthrough curve was obtained by integrating the plot of adsorbed concentration (C_{ad};mg L^{-1}) versus t (min). This can be used to calculate the quantity of tetracycline q_{total} (mg) retained in the column for a given inlet concentration and flow rate (Eq. (2)).

$$q_{total} = \frac{Q}{1000}\int_{t=0}^{t=t_{total}} C_{ad}\,dt = \frac{Q}{1000}\int_{t=0}^{t=t_{total}} (C_0 - C_t)dt \tag{2}$$

where C_0 and C_t are influent and effluent antibiotic concentrations (mg L^{-1}) respectively. Equilibrium adsorption capacity, q_{eq}(mg g^{-1}), is defined by Eq. (3) as the total amount of adsorbed (q_{total}) per dry weight of adsorbent in the column (w) at the end of process (Luo, Deng, Lin, & Zhang, 2011):

$$q_{eq} = \frac{q_{total}}{w} \tag{3}$$

The total amount of tetracycline (m_{total}) pumped into the column is obtained as following:

$$m_{total} = \frac{C_0 Q t_{total}}{1000} \tag{4}$$

And finally, the removal percentage of tetracycline from aqueous solution can be calculated as

$$Y = \frac{q_{total}}{m_{total}} \times 100 \tag{5}$$

2.5. Kinetic models of fixed bed column adsorption

In this study, data collected during laboratory tests were used as the basis for industrial applications. The rate of adsorption was studied by employing Adams–Bohart and Yoon–Nelson models to predict the dynamic behavior of fixed-bed column.

2.5.1. Adams–Bohart model

Adams–Bohart model is based on the surface reaction theory and describes the initial part of the breakthrough curve (Chu, 2010). The model equation is the following:

$$\ln\left(\frac{C_0}{C_t} - 1\right) = \ln\left(e^{k_{AB}N_0 Z/U_0} - 1\right) - k_{AB}\cdot C_0 \cdot t \tag{6}$$

where C_0 and C_t (mg L^{-1}) are the inlet and effluent tetracycline concentrations, k_{AB} (L mg^{-1} min^{-1}) is the mass transfer coefficient, t (min) is the service time, N_0 (mg L^{-1}) is the saturation concentration, U_0 (cm min^{-1}) is the linear velocity calculated by dividing the flow rate by the column cross-sectional area, and Z (cm) is the bed depth.

Because of much larger value of exponential term, this term can be simplified as:

$$e^{k_{AB}N_0 Z/U_0} - 1 \approx e^{k_{AB}N_0 Z/U_0} \tag{7}$$

And also the concentration ratio is considered to be low ($C_t \ll 0.1\,C_0$):

$$\ln\left(\frac{C_0}{C_t} - 1\right) = \ln\left(\frac{C_0 - C_t}{C_t}\right) \approx \ln\left(\frac{C_0}{C_t}\right) = -\ln\left(\frac{C_t}{C_0}\right) \tag{8}$$

Therefore the ultimate equation of Adams–Bohart model becomes (Trgo, Medvidovic, & Peric, 2011):

$$\ln\left(\frac{C_t}{C_0}\right) = k_{AB}C_0 t - k_{AB}N_0\frac{Z}{U_0} \tag{9}$$

The model parameters are obtained from the intercept and slope of a linear plot of $\ln(C_t/C_0)$ against t.

2.5.2. Yoon–Nelson model

Yoon and Nelson developed a relatively simple theoretical model. Theory of this model is: the rate of probability decrease in adsorption for each adsorbate molecule is proportional to the probability of the adsorbate adsorption and the probability of adsorbate breakthrough on the adsorbent (Yoon & Nelson, 1984). With considering A and P as the fractions of adsorbed solute in the bed, and the fraction of remained drug in the effluent respectively, the model equation for a single component system can be written as follows:

$$-\frac{dA}{dt} = k_{YN}.(t - \tau) \tag{10}$$

where k_{YN} (min^{-1}) is the rate velocity constant, and τ (min) is the time required for 50% adsorbate breakthrough (i.e. $C_t/C_0 \approx 0.5$). With replacing $P = 1 - A$ and considering $A = 0.5$ at time τ as the

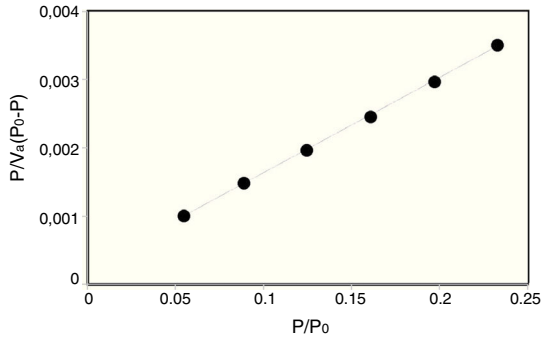

Fig. 2. Applying BET equation for calculating of specific surface area.

initial condition, integration of Eq. (10) gives the final form of Yoon–Nelson model:

$$\ln\left(\frac{C_t}{C_0 - C_t}\right) = k_{YN}t - \tau k_{YN} \tag{11}$$

From the linear dependence of $\ln[C_t/(C_0 - C_t)]$ versus t, the model parameters can be determined.

3. Results and discussion

3.1. Characterization of adsorbent

The yield of activated carbon was calculated and the value obtained was 26.16%. The experimental data of N_2 adsorption–desorption were plotted based on $P/V_a(P_0 - P)$ versus P/P_0 (Fig. 2), which shows a linear part in the initial region. The specific surface area can be calculated using slope and intercept of BET equation in the relative pressure range of $0.05 \leq P/P_0 \leq 0.25$, which is extensively reported in literature (Xu, Cheng, Cao, & Yu, 2015; Yu, Wang, Low, & Xiao, 2013); this range is used because of its closeness to completed monolayers. In other words, the most accurate measurement of specific surface area happens when only one layer of N_2 molecules occupy the interior pores of material. Therefore, this range was chosen because of providing high probability of monolayer adsorption in the lower relative pressures. Furthermore, the selection of the relative pressure range should fulfill two different criteria: first, the linear portion should have a positive intercept value; otherwise the obtained parameters would be meaningless. Second, the term $V_m(P_0 - P)$ has to constantly increase by increasing P/P_0. However these criteria limit the whole relative pressure range to the mentioned range ($0.05 \leq P/P_0 \leq 0.25$) and seems logical and consistent, it cannot be claimed that it is able to calculate the actual specific surface area (Rouquerol, Llewellyn, & Rouquerol, 2007).

Consequently, after obtaining the slope (s) and intercept (i) of the linear part in the mentioned range, monolayer volume (v_m) and constant (C) are determined. Afterwards, the specific surface area is calculated as follows: $S_{BET} = (v_m/V)N_A \cdot A_x/w = 307.603\ m^2\ g^{-1}$; Where v_m is the monolayer volume, V is the molar volume of nitrogen ($34.65\ cm^3\ mol^{-1}$), N_A is the Avogadro's number (6.022×10^{23}), A_x is the cross-sectional area of liquid nitrogen at 77 K ($0.162\ nm^2$) and w is the sample weight. Total pore volume, as the volume of adsorbed liquid nitrogen at $P/P_0 = 0.95$, was obtained $0.443\ cm^3\ g^{-1}$, consisted of 61% mesopores, and 39% micropores. The average pore diameter of prepared activated carbon was calculated 1.957 nm by BJH equation. According to International Union of Pure and Applied Chemistry (IUPAC) classification, the shape of N_2 adsorption–desorption isotherms demonstrated type II, which is known as having high percentage of mesopores; this is in agreement with the data mentioned above. The nanoporous materials are categorized into three types: micropores (<2 nm diameter), mesopores (2–50 nm diameter) and macropores (>50 nm diameter).

FE-SEM micrographs in Figure 3 show the surface morphology of the precursor and derived activated carbon. Large and well-developed pores on the surface of the activated carbon reveals the dehydrating action of the activation agent which resulted in more adsorption. In other words, phosphoric acid created a well-connected network of pores in the adsorbent particles during activation process, and tremendously increased the number of active site for adsorbing tetracycline molecules. It is worth mentioning that every adsorption process involves three main steps: First, migration of solute molecules from the solution to the boundary layer of adsorbent particle (known as external mass transfer). Second, diffusion of adsorbate molecules to the surface and interior pores of adsorbent particles (intra-particle diffusion). Third, physical or chemical attachment of these penetrated molecules to the active sites (adsorption). Accordingly, the more adsorption sites, the higher adsorption capacity.

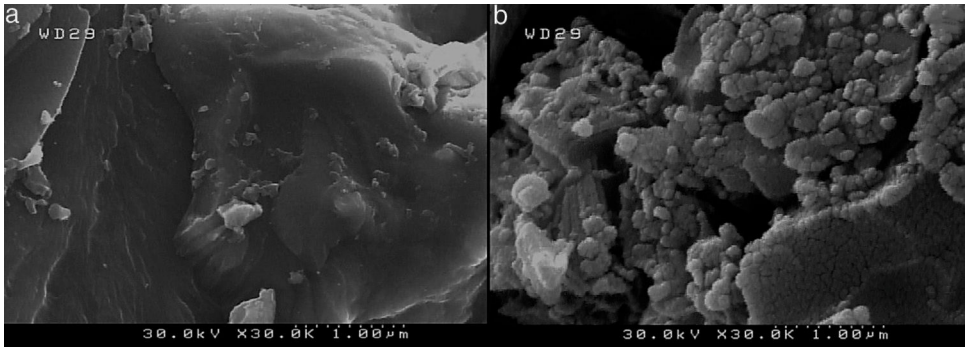

Fig. 3. FE-SEM images of: (a) precursor and (b) derived adsorbent.

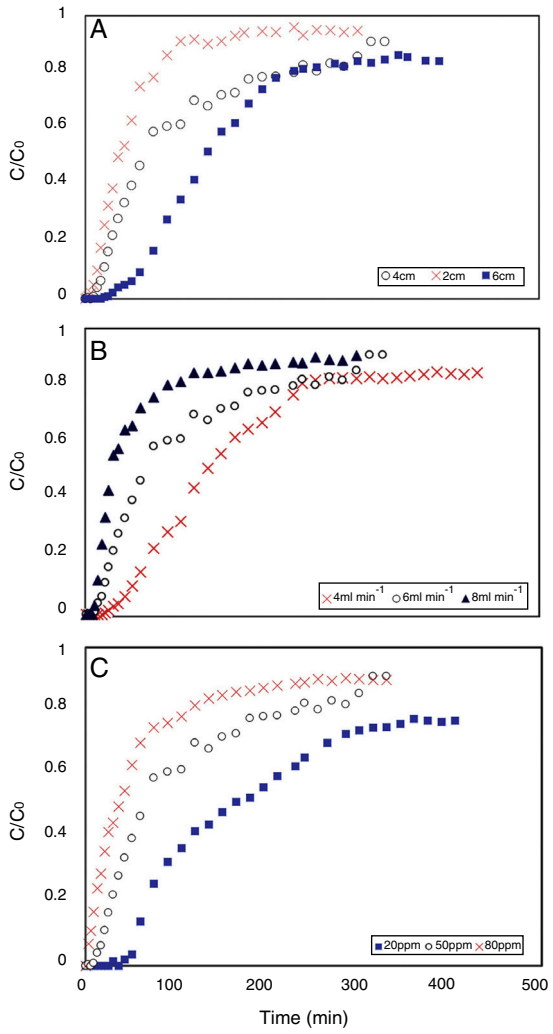

Fig. 4. Effect of (a) bed height, (b) flow rate, and (c) influent concentration on the breakthrough curve of tetracycline adsorption in the column. The process conditions were: $T = 298$ K and pH = 5.

3.2. Effect of bed height

Figure 4(a) shows a typical S-shape graph, known as breakthrough curve, obtained for adsorption of tetracycline on the activated carbon for different bed heights of 2, 4 and 6 cm (corresponding to 0.238, 0.477 and 0.715 g of adsorbent), at a constant flow rate of 6 mL min^{-1} and inlet concentration of 50 mg L^{-1}. The parameters in fixed bed column for tetracycline adsorption by produced adsorbent are listed in Table 2. From Figure 4(a), both breakthrough time (the time that $C_t/C_0 = 0.05$) and effluent volume increased with raising the bed depth. There is a term in continuous adsorption experiment so-called "exhaust time", which is a time that adsorbent can no longer remove solute molecules, and the influent solution leaves the experimental column without any considerable treatment. This criterion is considered $C_t/C_0 = 0.9$ in this study. According to the Figure 4(a), the exhaust time of 2, 4 and 6 cm bed depth was 100, 320 and 520 min (not shown in Fig. 4(a)), respectively. It increased with increasing bed height; because the higher bed depth means more adsorbent particles, or in other words more active sites for adsorption. With respect to the identical influent concentration and feed flow rate, When the bed depth increases, the adsorbate molecules have more time to diffuse into the pores of the adsorbent particles which led to increase in the number of tetracycline molecules adsorbed by the adsorbent (Taty-Costodes, Fauduet, Porte, & Ho, 2005). Accordingly, effluent volume ($V_{eff} = Q \cdot t_{exh.}$) is increased by increasing exhaust time, as a consequence of higher bed depth.

Interestingly, the adsorption capacity of tetracycline decreased with increasing the bed height, as it can be seen in Table 2 (rows: 1, 2 and 3). Although higher bed height provides more total surface area of adsorbent, the adsorption capacity (q_{eq}) of tetracycline decreases; the decrease of adsorption capacity can be simply justified by two main reasons: First, all binding sites were not accessible to adsorbate molecules in higher bed height (due to overlap of active sites), and as a result, some of these particle were not effectively used (Wang, Yu, Pan, & Xing, 2009). Second, due to the channeling effect, the solution usually finds its way to crawl near the column wall, which there is more voidage, even though glass wool layer was used for liquid distribution. It is worthwhile to mention that the entire capability of adsorbent should be utilized so that it could be applied for industrial applications (the significance of adsorption capacity concept). Therefore, lower bed depth was favorable to tetracycline adsorption capacity, which was in agreement with those referred by other authors (Chen et al., 2012; Luo et al., 2011).

3.3. Effect of flow rate

The effect of flow rate on the tetracycline adsorption in the column was investigated at bed height of 4 cm and inlet concentration of 50 mg L^{-1}. The adsorption breakthrough curves obtained at different flow rates are shown in Figure 4(b). It was observed that an increase in flow rate significantly reduced

Table 2
Process conditions and results for the fixed bed experiments ($T = 298$ K and pH = 5).

No.	Z (cm)	Q (mL min^{-1})	C_0 (mg L^{-1})	t_b (min)	m_{total} (mg)	q_{total} (mg)	q_{eq} (mg g^{-1})	Y (%)
1	2	6	50	9	90	17.57	73.72	19.53
2	4	6	50	15	99	34.33	71.99	34.68
3	6	6	50	43	117	49.96	69.83	42.70
4	4	4	50	39	96	36.70	76.97	38.23
5	4	8	50	9	120	20.84	43.72	17.37
6	4	6	20	55	48.6	23.84	50.00	49.05
7	4	6	80	2	144	35.94	75.37	24.95

Table 3
Comparison of the highest bed capacity of the prepared activated carbon with similar works in the literature.

Adsorbent	Adsorbate	Z (cm)	Q (mL min^{-1})	C_0 (mg L^{-1})	$q_{e,max}$ (mg g^{-1})	Reference
Apricot shell	Tetracycline	4	4	50	76.97	Present work
Oil palm shell	Methylene blue	6	20	100	40.86	Tan, Ahmad, & Hameed (2008)
Bamboo	Disperse orange 30	8	10	100	39.97	Ahmad, Idris, & Hameed (2014)
Bamboo waste	Reactive black 5	8	10	100	39.02	Ahmad and Hameed (2010)
Rice husk	Cu (II)	8	10	10	34.56	Yahaya, Abustan, Latiff, Bello, & Ahmad (2011)
Bamboo-charcoal	Tetracycline	2	6.6	50	23.50	Liao et al. (2013)

Table 4
Parameters of kinetic models using linear regression analysis.

Z (cm)	Q (mL min^{-1})	C_0 (mg L^{-1})	Adams–Bohart			Yoon–Nelson		
			k_{BA} (L mg^{-1} min^{-1})	N_0 (mg L^{-1})	R^2	k_{YN} (min^{-1})	τ (min)	R^2
2	6	50	0.1107	38.710	0.9953	0.0209	81.88	0.6765
4	6	50	0.1316	13.908	0.9239	0.0170	143.73	0.6844
6	6	50	0.1660	4.606	0.9946	0.0162	195.13	0.8006
4	4	50	0.1659	4.937	0.9917	0.0114	213.45	0.7341
4	8	50	0.1248	25.879	0.9999	0.0117	45.72	0.6275
4	6	20	0.2447	0.712	0.9999	0.0122	224.61	0.7391
4	6	80	0.0387	29.203	0.9999	0.0114	57.88	0.7401

the breakthrough time and adsorption capacity. This could be explained by the fact that at higher flow rate, tetracycline molecule had less time to diffuse into the adsorbent pores (Ahmad & Hameed, 2010). In other words, the residence time of the adsorbate in the column was not long enough to reach adsorption equilibrium at the given flow rate, and as a result, tetracycline molecules left the column without having the chance to reach the active sites of adsorbent particles. Furthermore, it is highly probable that high flow rate might desorb some of adsorbed tetracycline molecules with reversible and loose bond to the adsorbent surface. Therefore the tetracycline concentration in the effluent increased rapidly and resulted an earlier breakthrough time (Chen et al., 2012). Accordingly, the low flow rate was beneficial to tetracycline adsorption in the fixed bed, because of its higher adsorption capacity. These results were in agreement with those reported in previous studies (Han et al., 2009; Lignin et al., 2012). Bed capacity, breakthrough time and other parameters at different flow rates are presented in Table 2 (rows: 2, 4 and 5). The highest bed capacity of the prepared carbon in the present study is compared with similar works, which used activated carbon in eliminating tetracycline and other emerging pollutants. However there are a few works on continuous adsorption of tetracycline, Table 3 demonstrates that the tetracycline adsorption capacity in the present study is much higher than the capacity of other fixed bed adsorption processes in the literature.

3.4. Effect of influent concentration

The effect of different influent tetracycline concentration from 20 to 80 mg L^{-1} at constant adsorbent bed height of 4 cm and solution flow rate of 6 mL min^{-1} is illustrated in Figure 4(c). As expected, in higher influent concentration the adsorption process reached saturation faster and the breakthrough time was found to decrease from 55 to 2 min (Table 2, rows: 2, 6 and 7). This suggests that the change of concentration affects the saturation rate and breakthrough curve. This can be due to the fact that the greater concentration gradient causes a higher driving force for the mass transfer of tetracycline molecules, and consequently the adsorption sites will be covered more quickly (Liao et al., 2013). The driving force in adsorption process is the concentration difference between the antibiotics in the solution and the antibiotics on the surface of adsorbent (Aksu & Gönen, 2004). Therefore the high driving force due to the high tetracycline concentration led to a better column performance. Also, it was observed that the adsorption capacity was not proportionally increased with increasing influent concentration. As a result, adsorption capacity of tetracycline was higher when inlet concentration increased.

3.5. Evaluation of applied kinetic models

The empirical models by Adams–Bohart and Yoon–Nelson were utilized for mathematical simulation of experimental data in a continuous adsorption process. Adams–Bohart model was first used for gaseous application and recently has been employed to apply for liquid involved processes. With respect to Eq. (9), obtained in low concentration range, parameters of this model should be assigned to the initial part of breakthrough curve. The results for Adams–Bohart model parameters and related coefficients of correlation, R^2, values are shown in Table 4. High R^2 values show a good fitting of the model to the experimental data. The initial part of process is dominantly controlled by intra-particle diffusion mechanism. This is because of extremely high concentration driving force in liquid–solid mass transfer, which provides relatively high external mass transfer; therefore, intra-particle diffusion mechanism would control the process at initial part, due to its lower rate.

It is already pointed out in (Bohart & Adams, 1920), a good fitting of Adams–Bohart model to the adsorbate transport in the fixed bed column indicates that the surface diffusion was the rate-limiting step in the adsorption process. The saturation concentration, N_0, defined as the final effluent concentration predicted by this model, decreased with increasing bed height, but increased with increasing influent concentration and flow rate. At the identical process time, most of the tetracycline molecules were adsorbed in higher bed depth, and as a result would show much lower effluent concentration. Higher flow rate results in a higher effluent concentration; this is because a large number of molecules leave the column without treatment. According to the limited active sites of adsorbent particles, they are unable to embed all TC molecules in their pores at high concentrations, and therefore causes a higher N_0 in higher C_0. Despite the well-fitting of this model, it can be only used for the initial region of curve (C_t/C_0 less than 0.1).

The parameters of Yoon–Nelson model for investigation of breakthrough curve are shown in Table 4. The 50% breakthrough time, τ, significantly increased as bed height increased, which may be due to increased adsorbent surface area and more binding sites for adsorption (Kumar & Chakraborty, 2009). With the increase in flow rate, the values of τ decreased, which can be attributed to the rapid saturation of bed in higher flow rates. As can be seen in Table 4, higher inlet concentrations led to lower τ, which is due to the fact that higher driving force led to the faster occupation of active sites and therefore, a decrease in breakthrough time. However, these results seem reasonable and are totally in agreement with the changes in experimental data of $t_{b.}$ and $t_{exh.}$, it should be noted again that because of low R^2 values, this model is not reliable.

Accordingly, in order to model the transient stage or working stage of the breakthrough curve another model should be applied. Similar procedure was followed in a study about adsorption of methylene blue on phoenix tree leaf powder (Han et al., 2009).

3.6. Application of adaptive neuro-fuzzy inference system

Fuzzy systems can qualitatively express uncertainty and at the same time can have an exact performance, which is so-called computing with words in scientific literature. Furthermore, these systems can use human knowledge in their structures, which is expressed in the form of *if − then* rules (Mandal, Sahu, Giri, & Patel, 2014). Therefore the experience of professionals is used in various applications to create and design fuzzy systems. This specific feature of these systems is unique for fuzzy logics and artificial neural networks do not have it. The learning capabilities of neural network (followed the patterns of available data) can be combined to the fuzzy system (expressed qualitatively) so that a new hybrid intelligent system, called neuro-fuzzy system could be developed. The most known model proposed in this field is Adaptive Neuro-Fuzzy Inference System or ANFIS (Roohian, Abbasi, Hosseini, & Jahanmiri, 2014). Figure 5 shows a typical ANFIS structure which consists of five distinct layers.

A fuzzy model named first-order Takagi–Sugeno is considered with two inputs x and y and one output f. Typical fuzzy rules are the following:

$$\textit{Rule } i : \textit{if } x \textit{ is } A_i \textit{ and } y \textit{ is } B_i \quad \textit{then}$$
$$f_i = p_i x + q_i y + r_i; \quad i = 1, 2 \tag{12}$$

where A_i and B_i are the fuzzy sets, and p_i, q_i and r_i are the design parameters that are determined during the training process. The total output is the weighted average of outputs. The O_j^i represents the output of ith node in layer j (Mandal, Mahapatra, & Patel, 2015).

First layer (fuzzy layer): every single node in this layer generates a fuzzy membership grade.

$$O_i^1 = \mu_{A_i}(x) \quad i = 1, 2 \tag{13}$$

$$O_i^1 = \mu_{B_i}(y) \quad i = 1, 2 \tag{14}$$

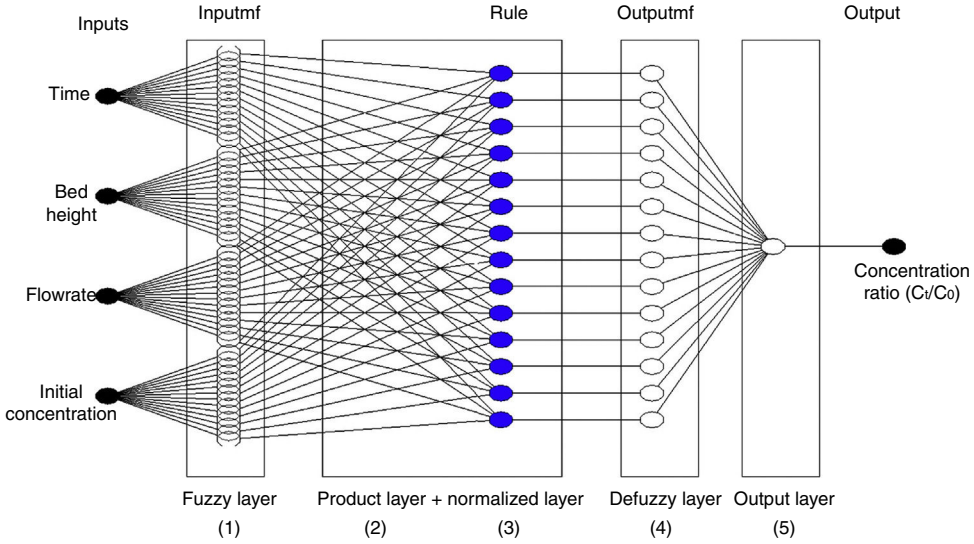

Fig. 5. Structure of ANFIS system in fixed-bed adsorption.

where $\mu_{A_i}(x)$ and $\mu_{B_i}(y)$ can adopt any fuzzy membership function. x (or y) is the input of node and A_i (or B_i) is the related fuzzy set. The Gaussian membership functions would be:

$$\mu_{A_i}(x) = \exp\left(-\frac{1}{2}\left(\frac{x - c_i}{a_i}\right)^2\right) \tag{15}$$

where c_i and a_i are the parameters that change the center and width of the membership function, respectively. In general, the output of this layer is the shape of membership function.

Second layer (product layer): the input membership grades analyze the firing strength of each rule via multiplication:

$$O_i^2 = w_i = \mu A_i(x) \times \mu B_i(y), \quad i = 1, 2 \tag{16}$$

where w_i is the firing strength of each rule.

Third layer (normalized layer): a normalization function is applied to obtain outputs as:

$$O_i^3 = \bar{w}_i = \frac{w_i}{w_1 + w_2}, \quad i = 1, 2 \tag{17}$$

where $\bar{w}_i$ is called normalized firing strength.

Forth layer (defuzzy layer): every node has the following function:

$$O_i^4 = \bar{w}_i f_i = \bar{w}_i(p_i + q_i y + r_i) \tag{18}$$

Finally, the fifth layer (total output layer): the overall output is computed by the aggregation of all incoming signals, i.e.

$$O_i^5 = \text{total output} = \sum_i^n \bar{w}_i f_i = \frac{\sum_i w_i f_i}{\sum_i w_i}, \quad i = 1, 2 \tag{19}$$

In the present study, a classical fuzzy model on the basis of the subtractive clustering algorithm was developed to predict the behavior of breakthrough curve. All subsequent processing and modeling were carried out using Matlab software and associated tools. Accordingly, 216 experimental data sets with 5 characteristics (4 inputs and 1 output) were used in this model: time, bed height, flow rate and initial concentration were considered as input attributes and concentration ratio (C_t/C_0) as target parameter. 90% of data sets were arbitrarily selected for training stage, and another subset consisted of 10% of data sets left for validation step.

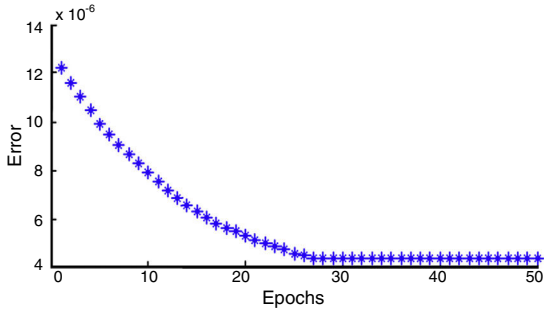

Fig. 6. Optimum number of training stages in ANFIS system.

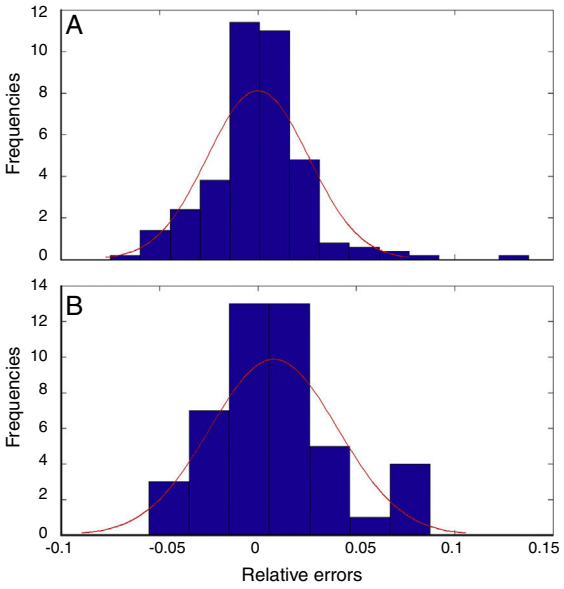

Fig. 7. Error graph in prediction of (a) training data and (b) testing data.

Takagi–Sugeno fuzzy structure was used based on Subtractive Clustering method with a radius of 0.6 for each cluster, and finally 21 fuzzy rules were obtained. Gaussian type membership functions were selected by the minimum and maximum values of 0 and 1, respectively. The back-propagation learning rule applied in this model is the same method which is used in common feed-forward neural networks. Figure 6 shows the training error versus number of epochs. As can be seen in this figure, overtraining occurred after stage 28 which means further training was ineffectual; nevertheless the number of stages was considered 50 to ensure of sufficient training.

Initially, the chosen training data were used to design a model for 50 stages. Afterwards in order to evaluate the prediction accuracy, the training and testing data were subjected to the model separately and their error graphs were determined, which can be seen in Figure 7(a) and (b) respectively. The perfect fit between the predicted output and experimental data sets introduces a promising method for modeling of continuous adsorption processes. Subsequently in order to validate the proposed model, some of the ANFIS predicted values and related experimental data sets were compared in Figure 8. The prediction accuracy was about 84% which presents excellent correlation between the experimental and predicted values. The variation pattern in training and testing phase is also presented in Figure 9. In this graph, the black dots represent experimental data and red dots indicate predicted values. According to the axis of this graph, all points should be placed on the line $y = x$ in the case of perfect prediction. Any Deviations from the line $y = x$ indicate modeling errors. To sum it up, the presented results confirm the well prediction of fixed-bed adsorption data by ANFIS model.

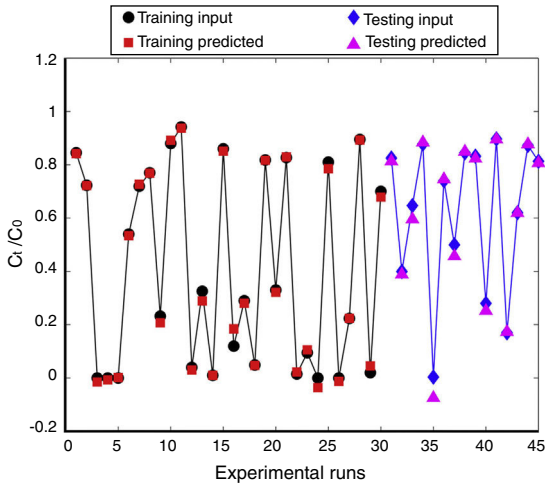

Fig. 8. Experimental runs versus predicted values for training and testing data.

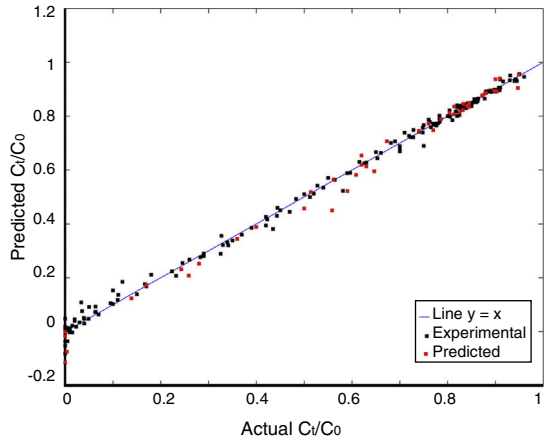

Fig. 9. Correlation plot of actual versus predicted data in training and testing phases.

4. Conclusion

This study presented a granular nanoporous activated carbon prepared from apricot shell by chemical activation using phosphoric acid, which was a promising adsorbent for an efficient removal of tetracycline in a fixed-bed adsorption column. The adsorption capacity of tetracycline was found to increase with increase in influent concentration but decrease with increasing bed height and feed flow rate. Three different models were used to describe the breakthrough curve: Yoon–Nelson equation was poorly fitted to the experimental data. Adams–Bohart model could satisfactorily describe only the initial section of breakthrough curve ($C_t \ll 0.1\, C_0$) at all experimental conditions. The proposed ANFIS model could perfectly predict the behavior of the curve at both parts, including the initial part and transient region. In conclusion, the obtained results of modeling confirm that presented ANFIS system can be taken into account for accurate modeling of continuous processes.

Conflict of interest

The authors have no conflicts of interest to declare.

Acknowledgements

The authors would like to thank Dr. Hossein Abolghasemi and anonymous reviewers for their valuable comments. The ceaseless supports of Mr. Seyed Mohammad Anvari and Mr. Seyed Hooman Anvari are also greatly appreciated.

References

Ahmad, A. A., & Hameed, B. H. (2010). Fixed-bed adsorption of reactive azo dye onto granular activated carbon prepared from waste. *Journal of Hazardous Materials*, *175*(1–3), 298–303. http://dx.doi.org/10.1016/j.jhazmat.2009.10.003

Ahmad, A. A., Idris, A., & Hameed, B. H. (2014). Modeling of disperse dye adsorption onto bamboo-based activated carbon in fixed-bed column. *Desalination and Water Treatment*, *52*(1–3), 248–256. http://dx.doi.org/10.1080/19443994.2013.794012

Aksu, Z., & Gönen, F. (2004). Biosorption of phenol by immobilized activated sludge in a continuous packed bed: Prediction of breakthrough curves. *Process Biochemistry*, *39*(5), 599–613. http://dx.doi.org/10.1016/S0032-9592(03)00132-8

Amiri, M. J., Abedi-Koupai, J., Eslamian, S. S., Mousavi, S. F., & Hasheminejad, H. (2013). Modeling Pb (II) adsorption from aqueous solution by ostrich bone ash using adaptive neural-based fuzzy inference system. *Journal of Environmental Science and Health, Part A*, *48*(5), 543–558. http://dx.doi.org/10.1080/10934529.2013.730451

Bohart, G. S., & Adams, E. Q. (1920). Some aspects of the behavior of charcoal with respect to chlorine. 1. *Journal of the American Chemical Society*, *42*(3), 523–544. http://dx.doi.org/10.1021/ja01448a018

Chen, S., Yue, Q., Gao, B., Li, Q., Xu, X., & Fu, K. (2012). Adsorption of hexavalent chromium from aqueous solution by modified corn stalk: A fixed-bed column study. *Bioresource Technology*, *113*, 114–120. http://dx.doi.org/10.1016/j.biortech.2011.11.110

Chen, C. Q., Zheng, L., Zhou, J. L., & Zhao, H. (2017). Persistence and risk of antibiotic residues and antibiotic resistance genes in major mariculture sites in Southeast China. *Science of the Total Environment*, *580*, 1175–1184. http://dx.doi.org/10.1016/j.scitotenv.2016.12.075

Chu, K. H. (2010). Fixed bed sorption: Setting the record straight on the Bohart–Adams and Thomas models. *Journal of Hazardous Materials*, *177*(1), 1006–1012. http://dx.doi.org/10.1016/j.jhazmat.2010.01.019

Cole, W. J., Powell, K. M., & Edgar, T. F. (2012). Optimization and advanced control of thermal energy storage systems. *Reviews in Chemical Engineering*, *28*(2–3), 81–99. http://dx.doi.org/10.1515/revce-2011-0018

González-Pleiter, M., Gonzalo, S., Rodea-Palomares, I., Leganés, F., Rosal, R., Boltes, K., . . ., & Fernández-Piñas, F. (2013). Toxicity of five antibiotics and their mixtures towards photosynthetic aquatic organisms: Implications for environmental risk assessment. *Water Research*, *47*(6), 2050–2064. http://dx.doi.org/10.1016/j.watres.2013.01.020

Han, R., Wang, Y., Zhao, X., Wang, Y., Xie, F., Cheng, J., & Tang, M. (2009). Adsorption of methylene blue by phoenix tree leaf powder in a fixed-bed column: Experiments and prediction of breakthrough curves. *Desalination*, *245*(1), 284–297. http://dx.doi.org/10.1016/j.desal.2008.07.013

He, L. Y., Ying, G. G., Liu, Y. S., Su, H. C., Chen, J., Liu, S. S., & Zhao, J. L. (2016). Discharge of swine wastes risks water quality and food safety: Antibiotics and antibiotic resistance genes from swine sources to the receiving environments. *Environment International*, *92–93*, 210–219. http://dx.doi.org/10.1016/j.envint.2016.03.023

Kumar, P. A., & Chakraborty, S. (2009). Fixed-bed column study for hexavalent chromium removal and recovery by short-chain polyaniline synthesized on jute fiber. *Journal of Hazardous Materials*, *162*(2), 1086–1098. http://dx.doi.org/10.1016/j.jhazmat.2008.05.147

Larsson, D. G. J., de Pedro, C., & Paxeus, N. (2007). Effluent from drug manufactures contains extremely high levels of pharmaceuticals. *Journal of Hazardous Materials*, *148*(3), 751–755. http://dx.doi.org/10.1016/j.jhazmat.2007.07.008

Liao, P., Zhan, Z., Dai, J., Wu, X., Zhang, W., Wang, K., & Yuan, S. (2013). Adsorption of tetracycline and chloramphenicol in aqueous solutions by

bamboo charcoal: A batch and fixed-bed column study. *Chemical Engineering Journal*, *228*, 496–505. http://dx.doi.org/10.1016/j.cej.2013.04.118

Lignin, O. A., Albadarin, A. B., Mangwandi, C., Al-muhtaseb, A. H., Walker, G. M., Allen, S. J., & Ahmad, M. N. M. (2012). Modelling and fixed bed column adsorption of Cr (VI) onto. *Chinese Journal of Chemical Engineering*, *20*(3), 469–477. http://dx.doi.org/10.1016/S1004-9541(11)60208-5

Luo, X., Deng, Z., Lin, X., & Zhang, C. (2011). Fixed-bed column study for Cu^{2+} removal from solution using expanding rice husk. *Journal of Hazardous Materials*, *187*(1–3), 182–189. http://dx.doi.org/10.1016/j.jhazmat.2011.01.019

Mandal, S., Sahu, M. K., Giri, A. K., & Patel, R. K. (2014). Adsorption studies of chromium (VI) removal from water by lanthanum diethanolamine hybrid material. *Environmental Technology*, *35*(7), 817–832. http://dx.doi.org/10.1080/09593330.2013.852627

Mandal, S., Mahapatra, S. S., & Patel, R. K. (2015). Neuro fuzzy approach for arsenic (III) and chromium (VI) removal from water. *Journal of Water Process Engineering*, *5*, 58–75. http://dx.doi.org/10.1016/j.jwpe.2015.01.002

Martins, A. C., Pezoti, O., Cazetta, A. L., Bedin, K. C., Yamazaki, D. A. S., Bandoch, G. F. G., . . ., & Almeida, V. C. (2015). Removal of tetracycline by NaOH-activated carbon produced from macadamia nut shells: Kinetic and equilibrium studies. *Chemical Engineering Journal*, *260*, 291–299. http://dx.doi.org/10.1016/j.cej.2014.09.017

Marzbali, M. H., Esmaieli, M., Abolghasemi, H., & Marzbali, M. H. (2016). Tetracycline adsorption by H_3PO_4-activated carbon produced from apricot nut shells: A batch study. *Process Safety and Environmental Protection*, *102*, 700–709. http://dx.doi.org/10.1016/j.psep.2016.05.025

Marzbali, M. H., Mir, A. A., Pazoki, M., Pourjamshidian, R., & Tabeshnia, M. (2017). Removal of direct yellow 12 from aqueous solution by adsorption onto spirulina algae as a high-efficiency adsorbent. *Journal of Environmental Chemical Engineering*, *5*(2), 1946–1956. http://dx.doi.org/10.1016/j.jece.2017.03.018

Nazari, G., Abolghasemi, H., Esmaieli, M., & Pouya, E. S. (2016). Aqueous phase adsorption of cephalexin by walnut shell-based activated carbon: A fixed-bed column study. *Applied Surface Science*, *375*, 144–153. http://dx.doi.org/10.1016/j.apsusc.2016.03.096

Oguz, E. (2013). Fixed-bed column studies on the removal of Fe^{3+} and neural network modelling. *Arabian Journal of Chemistry*, *10*(3), 313–320. http://dx.doi.org/10.1016/j.arabjc.2014.10.008

Pirdashti, M., Curteanu, S., Kamangar, M. H., Hassim, M. H., & Khatami, M. A. (2013). Artificial neural networks: Applications in chemical engineering. *Reviews in Chemical Engineering*, *29*(4), 205–239. http://dx.doi.org/10.1515/revce-2013-0013

Rezaei, H., Rahmati, M., & Modarress, H. (2015). Application of ANFIS and MLR models for prediction of methane adsorption on X and Y faujasite zeolites: Effect of cations substitution. *Neural Computing and Application*, *28*(2), 301–312. http://dx.doi.org/10.1007/s00521-015-2057-y

Roohian, H., Abbasi, A., Hosseini, Z., & Jahanmiri, A. (2014). Comparative modeling and analysis of the mass transfer coefficient in a turbulent bed contactor using artificial neural network and adaptive neuro-fuzzy inference systems. *Separation Science and Technology*, *49*(10), 1574–1583. http://dx.doi.org/10.1080/01496395.2014.891238

Rouquerol, J., Llewellyn, P., & Rouquerol, F. (2007). Is the BET equation applicable to microporous adsorbents? *Studies in Surface Science and Catalysis*, *160*, 49–56. http://dx.doi.org/10.1016/S0167-2991(07)80008-5

Shacham, M., & Brauner, N. (2008). Preventing oscillatory behavior in error control for ODEs. *Computers & Chemical Engineering*, *32*(3), 409–419. http://dx.doi.org/10.1016/j.compchemeng.2007.02.012

Tan, I. A. W., Ahmad, A. L., & Hameed, B. H. (2008). Adsorption of basic dye using activated carbon prepared from oil palm shell: Batch and fixed bed studies. *Desalination*, *225*(1–3), 13–28. http://dx.doi.org/10.1016/j.desal.2007.07.005

Taty-Costodes, V. C., Fauduet, H., Porte, C., & Ho, Y.-S. (2005). Removal of lead (II) ions from synthetic and real effluents using immobilized Pinus sylvestris sawdust: Adsorption on a fixed-bed column. *Journal of Hazardous Materials*, *123*(1), 135–144. http://dx.doi.org/10.1016/j.jhazmat.2005.03.032

Trgo, M., Medvidovic, N. V., & Peric, J. (2011). Application of mathematical empirical models to dynamic removal of lead on natural zeolite clinoptilolite in a fixed bed column. *Indian Journal of Chemical Technology*, *18*(2), 123–131. http://hdl.handle.net/123456789/11621

Turan, N. G., & Ozgonenel, O. (2013). *The design and implementation of adsorptive removal of Cu(II) from leachate using ANFIS* (vol. 2013 (590267)) http://dx.doi.org/10.1155/2013/590267

Wang, Z., Yu, X., Pan, B., & Xing, B. (2009). Norfloxacin sorption and its thermodynamics on surface-modified carbon nanotubes. *Environmental Science & Technology*, *44*(3), 978–984. http://dx.doi.org/10.1021/es902775u

Xu, D., Cheng, B., Cao, S., & Yu, J. (2015). Enhanced photocatalytic activity and stability of Z-scheme Ag_2CrO_4-GO composite photocatalysts for organic pollutant degradation. *Applied Catalysis B: Environmental*, *164*, 380–388. http://dx.doi.org/10.1016/j.apcatb.2014.09.051

Xu, J. J., An, M., Yang, R., Tan, Z., Hao, J., Cao, J., . . ., & Cao, W. (2016). Determination of tetracycline antibiotic residues in honey and milk by miniaturized solid phase extraction using chitosan-modified graphitized multiwalled carbon nanotubes. *Journal of Agricultural and Food Chemistry*, *64*(12), 2647–2654. http://dx.doi.org/10.1021/acs.jafc.6b00748

Yahaya, N., Abustan, I., Latiff, M., Bello, O. S., & Ahmad, M. A. (2011). Fixed-bed column study for Cu(II) removal from aqueous solutions using rice husk based activated carbon. *International Journal of Engineering and Technology*, *11*(1), 248–252.

Yoon, Y. H., & Nelson, J. H. (1984). Application of gas adsorption kinetics I. A theoretical model for respirator cartridge service life. *American Industrial Hygiene Association Journal*, *45*(8), 509–516. http://dx.doi.org/10.1080/15298668491400197

Yu, J., Wang, S., Low, J., & Xiao, W. (2013). Enhanced photocatalytic performance of direct Z-scheme g–C_3N_4–TiO_2 photocatalysts for the decomposition of formaldehyde in air. *Physical Chemistry Chemical Physics*, *15*(39), 16883–16890. http://dx.doi.org/10.1039/C3CP53131G